J Solid State Electrochem (2015) 19:3131–3138
DOI 10.1007/s10008-015-2942-4

ORIGINAL PAPER

Synthesis of $V_2O_5 \cdot 1.6H_2O$/graphene composite and its application in supercapacitors

Zhen-Duo Geng[1] · **Yu-ping Wang**[2]

Received: 28 February 2015 / Revised: 26 April 2015 / Accepted: 22 June 2015 / Published online: 2 July 2015

Abstract $V_2O_5 \cdot nH_2O$/graphene composite is synthesized by self-assembly of $V_2O_5 \cdot 1.6H_2O$ nanobelts on the surface of graphene via a simple hydrothermal method. The structure and morphologies of the composites are characterized by thermogravimetry analyzer, x-ray diffraction, and scanning electron microscope, respectively. It's found that the $V_2O_5 \cdot 1.6H_2O$ nanobelts are in width of 90 nm and length of 1.5 μm. The electrochemical behaviors of the composites in supercapacitors are tested by cyclic voltammetry and galvanostatic charge/discharge in a three-electrode system in KCl aqueous solution. Three pairs of redox peaks and voltage plateaus are observed correspondingly in the cyclic voltammetry curves and galvanostatic charge/discharge curves. The hybrid capacitance of this composite reaches 579 F/g at current density of 1 A/g and decreases 21 % after 5000 cycles at 4 A/g.

Keywords Xerogel · Graphene · Nanobelts · Supercapacitors

Introduction

Supercapacitors are considered to be one of the most important energy storage systems due to its high power density, long cycle life, and good stability [1]. Two basic capacitances are distinguished in supercapacitors: electrical double-layer capacitance formed along the electrode/electrolyte interface and pseudocapacitance generated by a fast reversible faradic process of the active materials. Unfortunately, the supercapacitors based on pseudocapacitance often result in compromises of rate capability and reversibility due to the insulating active materials. To figure out this disadvantage, conductive supporters, such as polymer, carbon, carbon nanotube, and graphene, are employed to provide good electronic conductivity for the active materials and excellent electrochemical performances are reported [2–5].

$V_2O_5 \cdot nH_2O$ is considered to be an ideal supercapacitor material due to its high surface area and high variable valence state [6, 7]. However, its low electronic conductivity limits the large-scale application in energy storage. In order to enhance the electronic conductivity, $V_2O_5 \cdot nH_2O$ was deposited on different conductive supporter, and good energy density and power density were delivered [8–10]. These results show that the conductive supporter plays an important role in enhancing the capacitance of $V_2O_5 \cdot nH_2O$. Graphene, a two-dimensional carbon material with high surface area and excellent electronic conductivity, is a promising electrode material and component in composites in energy storage. Due to the similar layer structure with $V_2O_5 \cdot nH_2O$, graphene is considered to be an ideal substrate for $V_2O_5 \cdot nH_2O$.

The combination of the good conductivity of graphene and the idea capacitance of $V_2O_5 \cdot nH_2O$ would create a good supercapacitor material. Recently, Lee [11, 12] reported the synthesis of V_2O_5 nanobelts on graphene by one-step hydrothermal method at 120 °C for 24 h and at room temperature for 8 weeks. The synthesized composites showed excellent cyclic stability and the capacitance maintained 82 % after 5000 cycles. However, the synthesis time for the composite is very long due to the low treatment temperature. Also, the capacitance of the composite is not very high since the pseudocapacitance of V_2O_5 was observed only at 0.25 A/g. In order to shorten the synthesis time and improve the capacitance properties, $V_2O_5 \cdot nH_2O$/graphene composites are synthesized by self

✉ Zhen-Duo Geng
duogengzhen@163.com

[1] College of Physics and Information Engineering, Henan Normal University, Xinxiang, Henan 453007, China

[2] College of Physic, Xinxiang University, Xinxiang 453007, China

assembly in a graphite oxide solution under hydrothermal condition, and its application in supercapacitors is demonstrated in this paper.

Experiment

Materials preparation

Graphite oxide (GO) was prepared by Hummers' method as reference described [13]. Two grams natural graphite flakes (200 meshes, Sigma-Aldrich), 1 g sodium nitrate (99.0 %, Sinopharm Chemical Reagent Co., Ltd.aladin®), and 46 mL sulfuric acid (≥95.0 %, Sinopharm Chemical Reagent Co., Ltd.) were mixed and stirred for 15 min with an ice bath. Then, 6 g potassium permanganate (≥99.5 %, Sinopharm Chemical Reagent Co., Ltd.) was slowly added into the above suspension. After 20 min, the ice bath was removed and the suspension was stirring at room temperature for 30 min. Ninety-two milliliters deionized (DI) water was added dropwise to the suspension, causing a violent effervescence. The temperature was maintained above 98 °C for 30 min. The suspension was diluted by 280 mL of water and treated with 10 mL of 30 % H_2O_2 (30 %, Sinopharm Chemical Reagent Co., Ltd.) to reduce the unreacted potassium permanganate. The GO was washed successively with DI water by centrifugation several times to remove residual salts and acids. The obtained GO was sonicated to achieve a stable GO dispersion in DI water.

$V_2O_5{\cdot}1.6H_2O$/graphene composite was synthesized by a simple hydrothermal method. Typically, 0.18 g V_2O_5 powder (99.6 %, Sigma-Aldrich) was added into 60 mL above the GO solution with stirring, then 5 mL 30 % H_2O_2 was added into the solution, continued stirring for 20 min for the dissolution of V_2O_5. The obtained solution was transfer into stainless steel autoclave reactor and heated at 190 °C for 12 h. Precipitates were collected and dried at 50 °C for 12 h in the vacuum oven and the composite was obtained.

As comparison, GO solution was reduced via hydrothermal treatment in stainless steel autoclave reactor at 190 °C for 12 h. The obtained black precipitates were dried at 50 °C.

Characterizations

The H_2O and graphene content of the composite was characterized by thermogravimetry analyzer (Perkin-Elmer TGA) in the temperature range from 25 to 550 °C in N_2 and air atmosphere, respectively. The heating rate is 5 °C/min.

The structure of the synthesized composites was determined using X-ray diffraction (XRD, Bruker D8 advance diffractmeter, Cu-Ka radiation, 1.5406 Å) with a scanning speed of 0.02°/s between 2θ of 5° and 60°. The X-ray photoelectron spectroscopy (XPS) was performed with a Phobios 100 electron analyzer (SPECS GmbH) equipped with five channeltrons, using an unmonochromated Al KR x-ray source (1486.6 eV). The morphology of the synthesized composite was characterized by a Quanta-200 (FEI) scanning electron microscope (SEM) under the accelerating voltage of 5.00 kV.

Electrochemical tests

The electrochemical performance was characterized by cyclic voltammetry (CV) and galvanostatic charge/discharge on a Solartron® 1287 electrochemical workstation. All the tests were carried out in a three-electrode system in 1 M KCl aqueous solution with Pt foil as counter electrode, Ag/AgCl (0.1 M KCl) as reference electrode. To prepare the working electrode, the active materials (graphene, $V_2O_5{\cdot}nH_2O$ xerogel, and the as-prepared composite), Super P (99+%, Sigma-Aldrich), and poly (vinylidene fluoride) binder (Sigma-Aldrich) were dispersed in N-methylpyrrolidinone (99+%, Sigma-Aldrich) by a weight ratio of 8:1:1 to form uniform slurry. Then the slurry was coated on a nickel foam substrate and dried at 50 °C for 6 h under vacuum. The prepared electrode was pressed into thin sheets. The CV characterization was performed in voltage range from −0.2 to 0.8 V, while the scan rate is 5, 10, 20, 50, and 100 mV/s. The charge/discharge test is carried out between −0.2 and 0.8 V at current density of 1, 2, and 4 A/g. The long-term cycle was tested at 4 A/g for 5000 cycles.

Results and discussion

Scheme 1 shows a schematic illustration of the self-assembly of $V_2O_5{\cdot}1.6H_2O$ nanobelts on graphene. In the synthesis solution, graphite oxide is a negative charged species since a large number of functional group formed during oxidation process [13, 14]. The V (V) precursors, formed by dissolution of V_2O_5 powder in H_2O_2, are highly charged cations in solution [4]. Due to the electrostatic attraction, V precursors are absorbed on the surface of graphite oxide. During the hydrothermal process, the absorbed V precursors transform to xerogel seeds, and then more V species deposit to generate $V_2O_5{\cdot}1.6H_2O$ nanobelts. Simultaneously, graphite oxides are reduced to form graphene under the hydrothermal condition [7]. Finally, the $V_2O_5{\cdot}1.6H_2O$/graphene composite is obtained. It is noted that the synthesis of composite in our work relies on the electrostatic attraction between V_2O_5 xerogel and the graphite oxide and self-assembly of $V_2O_5{\cdot}1.6H_2O$ xerogel. Since the graphite oxide is highly negative charged while the graphene is neutral, it is considered that the

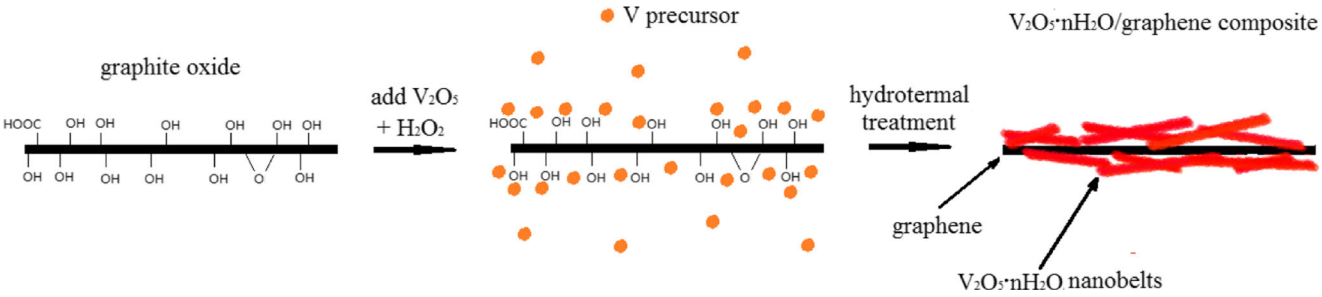

Scheme 1 Schematic illustration of the self-assembly of V_2O_5·nH_2O nanobelts on graphene

electrostatic attraction between V_2O_5 xerogel and the graphite oxide is stronger than that between V_2O_5 xerogel and the reduced graphene in literature [15]. Also, the solution is colorless after the hydrothermal synthesis indicating that all the V species are assembled on the graphene.

Figure 1 shows the thermogravimetric analysis (TGA) curves for the V_2O_5·nH_2O/graphene composite in N_2 and air atmosphere. In the N_2 atmosphere, as the temperature increases, the weight loss of the composite is about 5.7 % before 100 °C and 9.6 % until 310 °C. After 310 °C, the weight of the composite maintains consistent. This weight loss corresponds to the remove of weakly bound chemical water in the V_2O_5·nH_2O xerogel [15, 16]. In the air atmosphere, the weight loss profile is different from that in N_2 atmosphere after approximate 150 °C because of the oxidation of graphene. After the complete burn-off of graphene, 65.8 % of its initial weight which is the content of V_2O_5 is retained after 500 °C. The difference of the weight loss between the TGA curves in N_2 and air atmosphere at 550 °C is due to the burning of the graphene, thus the weight of graphene in this composite is approximate 30 %. The inset figure is the TGA curve of

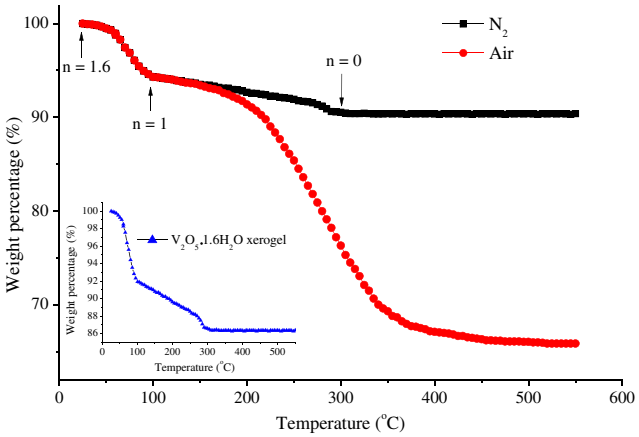

Fig. 1 TGA curves of the V_2O_5·1.6H_2O/graphene composite in N_2 and air atmosphere. The inset figure is the TGA curve of the V_2O_5·1.6H_2O xerogel in N_2 atmosphere. The temperature range is from 25 to 550 °C, and the heating rate is 5 °C/min

V_2O_5·nH_2O xerogel in N_2. The TGA curve of V_2O_5·nH_2O xerogel shows a similar profile with that of V_2O_5·nH_2O/graphene composite in N_2. After 300 °C, the V_2O_5·nH_2O xerogel shows a weight loss of 13.5 % due to the remove of H_2O in the xerogel. This weight loss indicates that the value of "n" in V_2O_5·nH_2O is 1.6.

Figure 2 displays the XRD patterns of the V_2O_5·1.6H_2O/graphene composite and the pure hydrothermal reduced graphene and V_2O_5·1.6H_2O xerogel. No sharp diffraction peak is observed in the XRD pattern of the pure graphene except a broad peak at 2θ of 27°. The broad peak at is due to the restack of graphene during reduction and drying process. In the XRD pattern of the composite, only a few peaks are distinguished at 2θ of 6.3°, 12.4°, 18.7°, and 25.2° which are similar with those of the V_2O_5·nH_2O xerogel identified as the (00l) reflection peaks of a layer structure [15, 17–19]. The d-spacing of the (001) reflection which is equivalent to the interlayer distance is about 14.2 Å, confirming the intercalation of H_2O molecule into the interlayer of V_2O_5. The absence of this broad peak at 27° in the XRD pattern of the composite suggests that the V_2O_5·1.6H_2O on the surface of graphene is conducive to prevent the restack of graphene during reduction. The peak intensity of the (001) reflection is much stronger than those of other (00l) reflections, indicating that the thickness of the assembled V_2O_5·1.6H_2O is very small, probably only a few layers [20]. This thin layer structure can greatly reduce the diffusion resistance and improve the utilization efficiency of V species in supercapacitors.

Figure 3 shows the C 1 s XPS spectrum of GO and the V_2O_5·1.6H_2O/graphene composite. For GO, two peaks are observed clearly. The sharp peak at approximate 284.5 eV is the sp^2 carbon corresponding to the C=C bond. The broad peak at 287.2 eV relates to the functional groups such as hydroxyl, epoxide, and carboxyl. After the hydrothermal treatment, the peak for functional groups decreases largely while the sp^2 carbon peak changes little. This suggests that most of the functional groups on GO were removed during the hydrothermal synthesis and the GO was reduced to graphene [21].

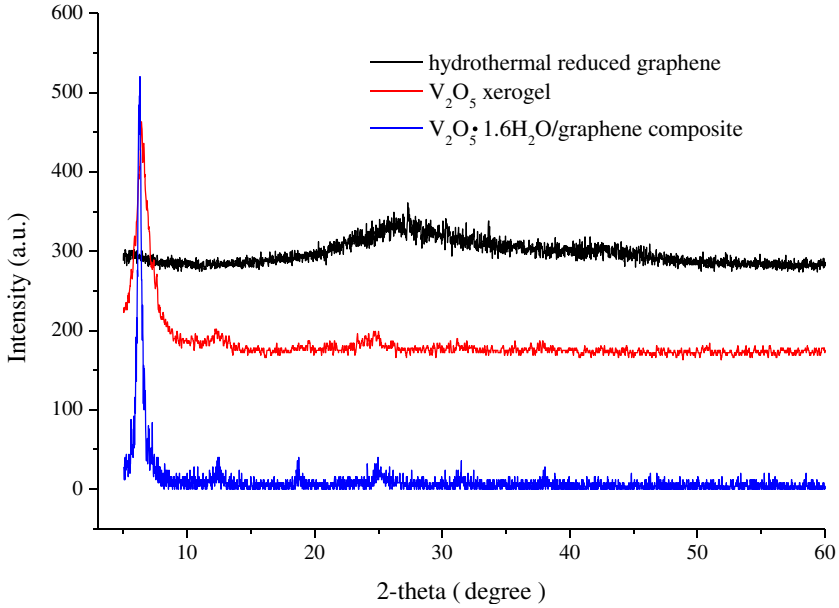

Fig. 2 XRD patterns of the hydrothermal reduced graphene, V_2O_5·nH_2O xerogel, and the V_2O_5·nH_2O/graphene composite

Figure 4 shows the SEM images of the synthesized V_2O_5·1.6H_2O/graphene composite and pure V_2O_5·1.6H_2O xerogel. In Fig. 4a, an overall image of the synthesized composite is presented. It can be seen that the composite is composed of a large number of curly sheets which is lead to a porous structure. In Fig. 4b, more details of the composite are observed. A large number of grass-like nanobelts cover on the surface of the sheet. From the sheets which are vertical to the image (at the top of the Fig. 4b), it can be seen that these nanobelts cover both sides of the sheet. This kind of structure confirms the synthesis mechanism described in Scheme 1. Due to the electrostatic attraction, the V precursor is absorbed on the surface of the negative charged graphite oxide to generate V_2O_5·nH_2O nanobelts. In Fig. 4c, d, the self-assembled V_2O_5·nH_2O is clearly identified as nanobelts with width of 90 nm and length of 1.5 μm. These assembled nanobelts attach fast on the surface of graphene and stack together to form a porous structure. Such a structure is conducive to enhance the electronic conductivity of V_2O_5·1.6H_2O and enlarge area of the electrode/electrolyte interface and thus improve the electrochemical performance in supercapacitors [22]. In Fig.4e, f, the pure V_2O_5·1.6H_2O xerogel presents as an aggregation of a large number of nanowires. The difference on morphology is due that the pure V_2O_5·1.6H_2O xerogel is growth by free V species in the solution, while the V_2O_5·1.6H_2O/graphene composite is by absorbed V species on the surface of GO. This confirms that GO is conductive on the dispersion of V_2O_5·1.6H_2O xerogel. It also found that the morphology of the V_2O_5·1.6H_2O/graphene composite is difference from that in Lee's work [11, 12]. In Lee's work, the growth of V_2O_5·1.6H_2O via a long time and thus long nanowires was obtained. In this work, the V species were absorbed on the surface of GO, then transferred to V_2O_5·1.6H_2O nanobelt in a short time. One of the advantages is that the contact of V_2O_5·1.6H_2O xerogel and graphene is better in the latter one.

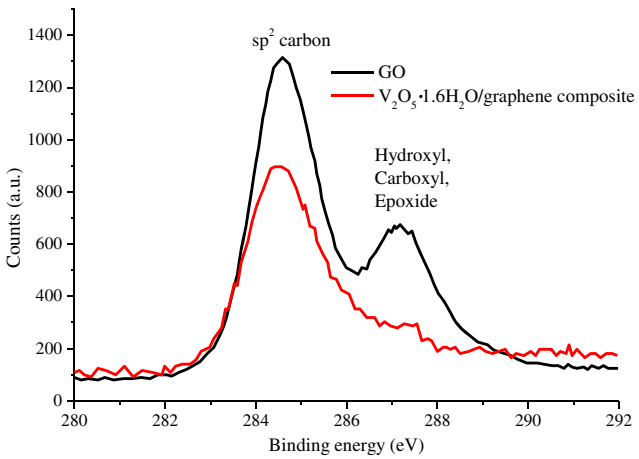

Fig. 3 **a** The C 1 s XPS spectrum of GO and the V_2O_5·1.6H_2O/graphene composite

CV experiments were carried out to characterize the electrochemical behavior of the V_2O_5·1.6H_2O/graphene composite for supercapacitors. Figure 5 presents the comparison of CV curves for pure graphene, V_2O_5·1.6H_2O xerogel, and the V_2O_5·1.6H_2O/graphene composite at scan rate of 20 mV/s. For graphene, only a nearly rectangular CV curve without any redox peak is observed, suggesting a pure electrical double-layer capacitance [23, 24]. In the CV curve of V_2O_5·

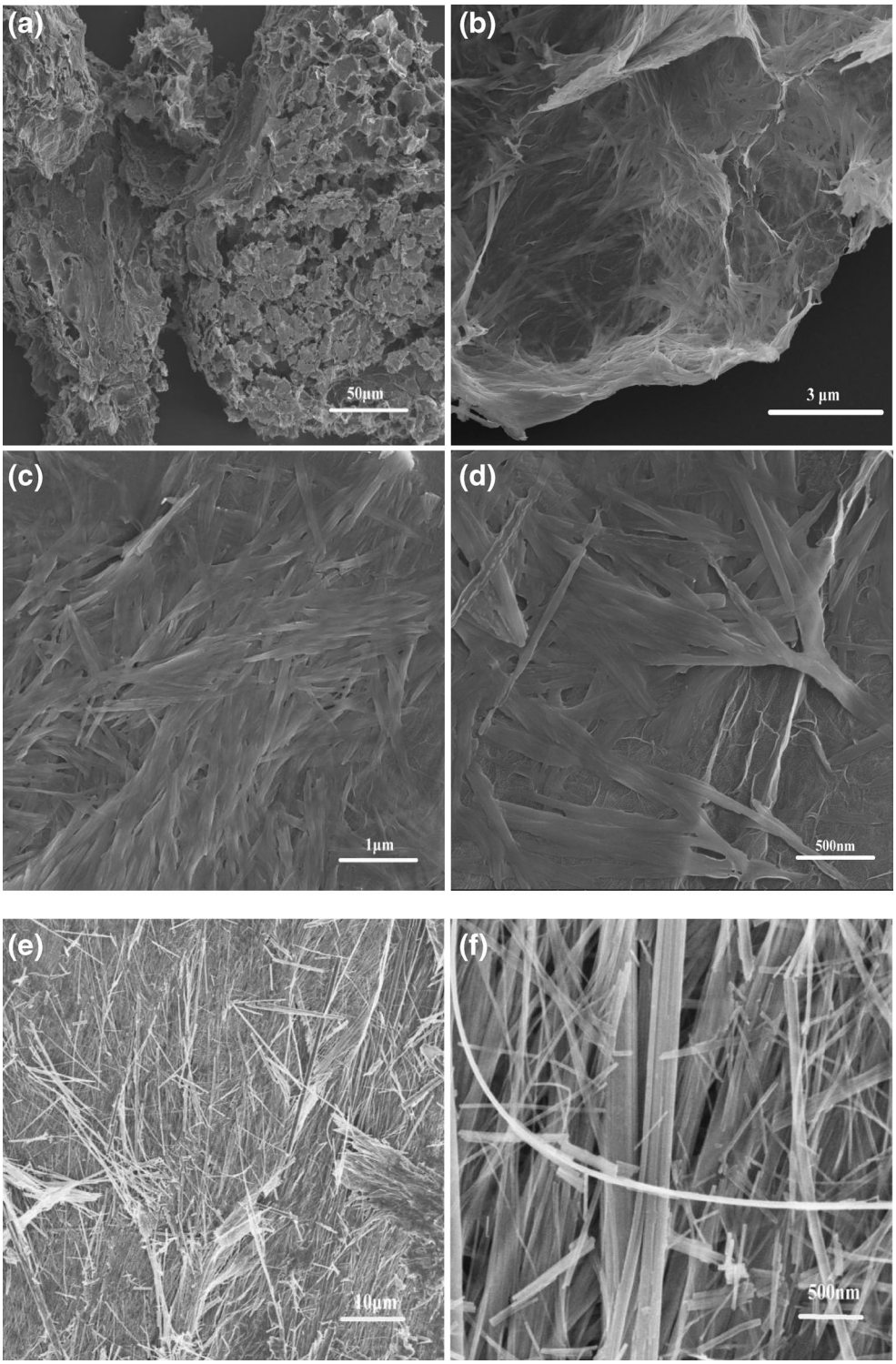

Fig. 4 SEM images of the $V_2O_5 \cdot 1.6H_2O$/graphene composite at different magnification (**a**, **b**, **c**, and **d**) and $V_2O_5 \cdot nH_2O$ (**e** and **f**)

$1.6H_2O$ xerogel, two pairs of redox peaks with weak intensity are observed, indicating a small faradic capacitance. This is due to its weak electronic conductivity of $V_2O_5 \cdot 1.6H_2O$ xerogel. In the CV curve of $V_2O_5 \cdot 1.6H_2O$/graphene composite, three pairs of redox peaks obviously in the CV curve. The anodic peaks locate at approximate 0.49, 0.19, and 0.11 V while the cathodic peaks at 0.36, 0.16, and 0.08 V, corresponding to the redox potential of V^{5+}/V^{4+},

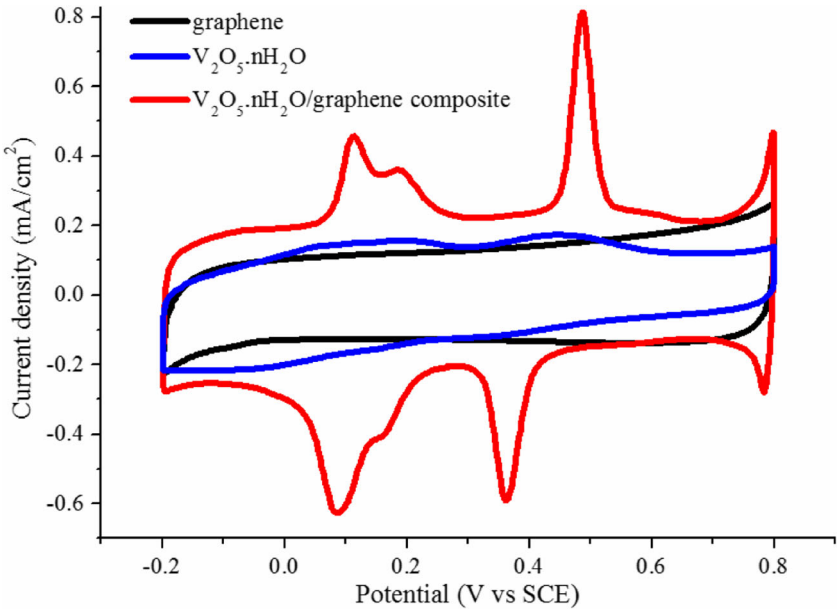

Fig. 5 CV curves of the hydrothermal reduced graphene, $V_2O_5{\cdot}nH_2O$ xerogel, and $V_2O_5{\cdot}nH_2O$ /graphene composite. The CV tests is performed in a three electrode system with Pt foil as counter electrode, Ag/AgCl (0.1 M KCl) as reference electrode and 1 M KCl aqueous solution as electrolyte. The voltage range is between −0.2 and 0.8 V and the scan rate is 20 mV/s

V^{4+}/V^{3+}, and V^{3+}/V^{2+}, respectively. The redox peaks, shown good symmetry in the CV curves, indicate a reversible faradic process [25]. As a results, the $V_2O_5{\cdot}1.6H_2O$/graphene composite exhibits a hybrid of electric double layer capacitance pseudocapacitance [26, 27]. It is believed that the presence of the distinguishable redox peaks is benefited from the physical structure of the composite. As discussed before, the $V_2O_5{\cdot}1.6H_2O$ xerogel in the morphology of nanobelt assembles on the surface of graphene to generate the composite. The graphene provides perfect electron conductivity, while the $V_2O_5{\cdot}1.6H_2O$ xerogel exhibit good pseudocapacitance. Combining these two advantages, the $V_2O_5{\cdot}1.6H_2O$/graphene composite shows good performance in supercapacitors.

Figure 6 shows the CV curves of the synthesized $V_2O_5{\cdot}1.6H_2O$/graphene composite at different scan rate. As the scan rate increases, CV curves show the same shape while the response current increases relatively. The redox peaks in the CV curves exhibit good mirror images with respect to the zero-the current line, revealing facile diffusion/transport of ions and good adsorption behavior [28, 29]. These results indicate that the composite possesses a good rate performance for supercapacitors.

In order to evaluate the supercapacitor performance of the as-prepared composite, galvanostatic charge/discharge tests are carried out in a three-electrode system. Typical charge/discharge curves for the $V_2O_5{\cdot}1.6H_2O$/graphene composite at current densities of 1, 2, and 4 A/g and its long-term cycle performance as well as that of $V_2O_5{\cdot}nH_2O$ xerogel are presented respectively in Fig. 7a, b. In Fig. 7a, voltage plateaus corresponding to the redox peaks in CV curves are identified clearly in the charge/discharge curves, and the IR drops for all the curves are not obvious. It should be mentioned that these distinguishable voltage plateaus of $V_2O_5{\cdot}1.6H_2O$ xerogel for supercapacitors are rarely reported previously [25, 7]. The plateaus, indicating the intercalation/deintercalation of K^+ into the $V_2O_5{\cdot}1.6H_2O$ lattice, are benefitted from the thin layer structure and the large interlayer distance of $V_2O_5{\cdot}1.6H_2O$ xerogel, as well as the good conductivity of the graphene supporter. As the current density increases, the voltage plateaus maintain constant, indicating a stable

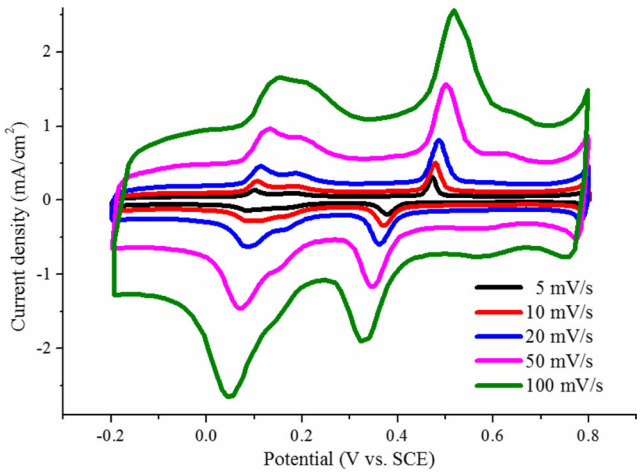

Fig. 6 CV curves of the $V_2O_5{\cdot}nH_2O$/graphene composite at different scan rate: 5, 10, 20, 50, and 100 mV/s. The CV tests are performed between −0.2 and 0.8 V with Pt foil as counter electrode, Ag/AgCl (0.1 M KCl) as reference electrode and 1 M KCl aqueous solution as electrolyte

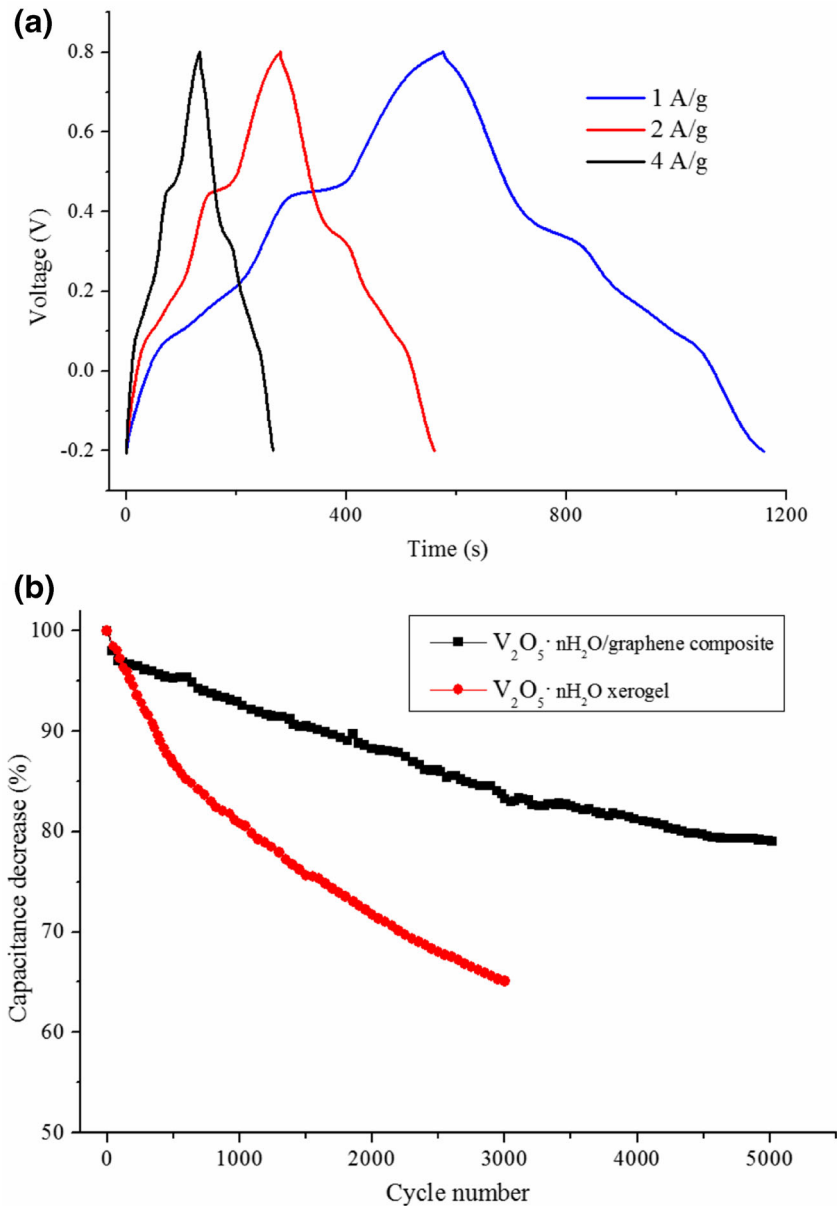

Fig. 7 **a** The galvanostatic charge/discharge curves of the $V_2O_5{\cdot}nH_2O$/graphene composite at different current density of 1, 2, and 4 A/g. **b** The comparison of capacitance decrease for the $V_2O_5{\cdot}nH_2O$ xerogel and the synthesized $V_2O_5{\cdot}nH_2O$/graphene composite for supercapacitor during long-term cycle at 4 A/g. The charge/discharge tests are performed between −0.2 and 0.8 V with Pt foil as counter electrode, Ag/AgCl (0.1 M KCl) as reference electrode, and 1 M KCl aqueous solution as electrolyte

pseudocapacitance. The specific capacitance of the composite reaches 579, 560, and 534 F/g at current density of 1, 2, and 4 A/g, respectively. In Fig. 7b, the capacitance of the $V_2O_5{\cdot}nH_2O$/graphene composite decreases 21 % after 5000 cycles at 4 A/g. As a comparison, the capacitance of $V_2O_5{\cdot}1.6H_2O$ xerogel reduces about 35 % after 3000 cycles. Since the electrolyte gradually turns into a yellow-green color, the dissolve of the active $V_2O_5{\cdot}1.6H_2O$ xerogel during charge/discharge process is considered to be the main reason for the capacitance loss [30]. It is believed that the loading of $V_2O_5{\cdot}1.6H_2O$ xerogel on the conductive supporter is helpful to prevent its dissolution.

Conclusion

By an easy hydrothermal method, $V_2O_5{\cdot}1.6H_2O$ nanobelts in width of 90 nm and length of 1.5 μm are self-assembled on the surface of graphene. Combining the faradic capacitance of $V_2O_5{\cdot}1.6H_2O$ xerogel and good conductivity of graphene, $V_2O_5{\cdot}1.6H_2O$/graphene composite shows much better electrochemical performance than pure graphene and $V_2O_5{\cdot}1.6H_2O$ xerogel in supercapacitors. Distinguishable redox peaks in CV curves and voltage plateaus in charge/discharge curves are observed in the electrochemical characterization, indicating a great contribution of pseudocapacitance to the overall

capacitance. The specific capacitance of the synthesized $V_2O_5{\cdot}1.6H_2O$/graphene composite reaches 579 F/g at current density of 1 A/g and reduces 21 % after 5000 cycles at 4 A/g. The main reason for the capacitance loss is the dissolution of the $V_2O_5{\cdot}1.6H_2O$ xerogel during charge/discharge process.

References

1. Conway BE (1999) Electrochemical supercapacitors: scientific, fundamentals, and technological applications. Kluwer, New York
2. Wu Z-S, Zhou G, Yin L-C, Ren W, Li F, Cheng H-M (2012) Graphene/metal oxide composite electrode materials for energy storage. Nano Energy 1(1):107–131
3. Wang H, Casalongue HS, Liang Y, Dai H (2010) $Ni(OH)_2$ nanoplates grown on graphene as advanced electrochemical pseudocapacitor materials. J Am Chem Soc 132(21):7472–7477
4. Li Z, Zhu Q, Huang S, Jiang S, Lu S, Chen W, Zakharova GS (2014) Interpenetrating network V_2O_5 nanosheets/carbon nanotubes nanocomposite for fast lithium storage. RSC Adv 4(87): 46624–46630
5. Bai M-H, Bian L-J, Song Y, Liu X-X (2014) Electrochemical codeposition of vanadium oxide and polypyrrole for high-performance supercapacitor with high working voltage. ACS Appl Mater Interfaces 6(15):12656–12664
6. Qu QT, Shi Y, Li LL, Guo WL, Wu YP, Zhang HP, Guan SY, Holze R (2009) $V_2O_5{\cdot}0.6H_2O$ nanoribbons as cathode material for asymmetric supercapacitor in K_2SO_4 solution. Electrochem Commun 11(6):1325–1328
7. Qu QT, Liu LL, Wu YP, Holze R (2013) Electrochemical behavior of $V_2O_5{\cdot}0.6H_2O$ nanoribbons in neutral aqueous electrolyte solution. Electrochim Acta 96:8–12
8. Kudo T, Ikeda Y, Watanabe T, Hibino M, Miyayama M, Abe H, Kajita K (2002) Amorphous V2O5/carbon composites as electrochemical supercapacitor electrodes. Solid State Ionics 152–153: 833–841
9. Kim I-H, Kim J-H, Cho B-W, Lee Y-H, Kim K-B (2006) Synthesis and electrochemical characterization of vanadium oxide on carbon nanotube film substrate for pseudocapacitor applications. J Electrochem Soc 153(6):A989–A996
10. Rui X, Zhu J, Liu W, Tan H, Sim D, Xu C, Zhang H, Ma J, Hng HH, Lim TM, Yan Q (2011) Facile preparation of hydrated vanadium pentoxide nanobelts based bulky paper as flexible binder-free cathodes for high-performance lithium ion batteries. RSC Adv 1(1): 117–122
11. Lee M, Hong WG, Jeong HY, Balasingam SK, Lee Z, Chang S-J, Kim BH, Jun Y (2014) Graphene oxide assisted spontaneous growth of V_2O_5 nanowires at room temperature. Nanoscale 6(19): 11066–11071
12. Lee M, Balasingam SK, Jeong HY, Hong WG, Lee H-B-R, Kim BH, Jun Y (2015) One-step hydrothermal synthesis of graphene decorated V_2O_5 nanobelts for enhanced electrochemical energy storage. Sci Rep 5:8151
13. Hummers WS, Offeman RE (1958) Preparation of graphitic oxide. J Am Chem Soc 80(6):1339–1339
14. Ramesha GK, Vijaya Kumara A, Muralidhara HB, Sampath S (2011) Graphene and graphene oxide as effective adsorbents toward anionic and cationic dyes. J Colloid Interface Sci 361(1): 270–277
15. Du G, Seng KH, Guo Z, Liu J, Li W, Jia D, Cook C, Liu Z, Liu H (2011) Graphene-$V_2O_5{\cdot}$nH2O xerogel composite cathodes for lithium ion batteries. RSC Adv 1(4):690–697
16. Ying Wang HS, Chou T, Cao G (2005) Effects of thermal annealing on the Li^+ intercalation properties of $V_2O_5{\cdot}nH_2O$ xerogel films. J Phys Chem B 109(22):5
17. Wu CG, DeGroot DC, Marcy HO, Schindler JL, Kannewurf CR, Liu YJ, Hirpo W, Kanatzidis MG (1996) Redox intercalative polymerization of aniline in V_2O_5 Xerogel. The postintercalative intralamellar polymer growth in polyaniline/metal oxide nanocomposites is facilitated by molecular oxygen. Chem Mater 8(8):1992–2004
18. Liu J, Wang X, Peng Q, Li Y (2005) Vanadium pentoxide nanobelts: highly selective and stable ethanol sensor materials. Adv Mater 17(6):764–767
19. Glynn C, Thompson D, Paez J, Collins G, Benavente E, Lavayen V, Yutronic N, Holmes JD, Gonzalez G, O'Dwyer C (2013) Large directional conductivity change in chemically stable layered thin films of vanadium oxide and a 1D metal complex. J Mater Chem C 1(36):5675–5684
20. Petkov V, Trikalitis PN, Bozin ES, Billinge SJL, Vogt T, Kanatzidis MG (2002) Structure of $V_2O_5{\cdot}nH_2O$ xerogel solved by the atomic pair distribution function technique. J Am Chem Soc 124(34): 10157–10162
21. Zhang LL, Zhao S, Tian XN, Zhao XS (2010) Layered graphene oxide nanostructures with sandwiched conducting polymers as supercapacitor electrodes. Langmuir 26(22):17624–17628
22. Liu Y, Li J, Zhang Q, Zhou N, Uchaker E, Cao G (2011) Porous nanostructured V_2O_5 film electrode with excellent Li-ion intercalation properties. Electrochem Commun 13(11):1276–1279
23. Liu C, Yu Z, Neff D, Zhamu A, Jang BZ (2010) Graphene-based supercapacitor with an ultrahigh energy density. Nano Lett 10(12): 4863–4868
24. Patil S, Patil V, Sathaye S, Patil K (2014) Facile room temperature methods for growing ultra thin films of graphene nanosheets, nanoparticulate tin oxide and preliminary assessment of graphene-tin oxide stacked layered composite structure for supercapacitor application. RSC Adv 4(8):4094–4104
25. Stojković I, Cvjetićanin N, Pašti I, Mitrić M, Mentus S (2009) Electrochemical behaviour of V_2O_5 xerogel in aqueous $LiNO_3$ solution. Electrochem Commun 11(7):1512–1514
26. Sugimoto W, Iwata H, Yasunaga Y, Murakami Y, Takasu Y (2003) Preparation of ruthenic acid nanosheets and utilization of its interlayer surface for electrochemical energy storage. Angew Chem Int Ed 42(34):4092–4096
27. Chen Z, Qin Y, Weng D, Xiao Q, Peng Y, Wang X, Li H, Wei F, Lu Y (2009) Design and synthesis of hierarchical nanowire composites for electrochemical energy storage. Adv Funct Mater 19(21):3420–3426
28. Yan J, Liu J, Fan Z, Wei T, Zhang L (2012) High-performance supercapacitor electrodes based on highly corrugated graphene sheets. Carbon 50(6):2179–2188
29. Chen Z, Wen J, Yan C, Rice L, Sohn H, Shen M, Cai M, Dunn B, Lu Y (2011) High-performance supercapacitors based on hierarchically porous graphite particles. Adv Energy Mater 1(4):551–556
30. Lee HY, Goodenough JB (1999) Ideal supercapacitor behavior of amorphous $V_2O_5{\cdot}nH_2O$ in potassium chloride (KCl) aqueous solution. J Solid State Chem 148(1):81–84